

## Evolution of the radio - X-ray coupling throughout an entire outburst of Aquila X-1

J. C. A. Miller-Jones<sup>1,15</sup>, G. R. Sivakoff<sup>2</sup>, D. Altamirano<sup>3</sup>, V. Tudose<sup>4,16,17</sup>, S. Migliari<sup>5</sup>, V. Dhawan<sup>6</sup>, R. P. Fender<sup>7,3</sup>, M. A. Garrett<sup>4,18,19</sup>, S. Heinz<sup>8</sup>, E. G. Körding<sup>9</sup>, H. A. Krimm<sup>10,20</sup>, M. Linares<sup>11</sup>, D. Maitra<sup>12</sup>, S. Markoff<sup>3</sup>, Z. Paragi<sup>13,21</sup>, R. A. Remillard<sup>11</sup>, M. P. Rupen<sup>6</sup>, A. Rushton<sup>7</sup>, D. M. Russell<sup>3</sup>, C. L. Sarazin<sup>2</sup>, R. E. Spencer<sup>14</sup>

jmillier@nrao.edu

### ABSTRACT

---

<sup>1</sup>NRAO Headquarters, 520 Edgemont Road, Charlottesville, VA 22902.

<sup>2</sup>Department of Astronomy, University of Virginia, P.O. Box 400325, Charlottesville, VA 22904

<sup>3</sup>Astronomical Institute ‘Anton Pannekoek’, University of Amsterdam, P.O. Box 94249, 1090 GE Amsterdam, the Netherlands

<sup>4</sup>Netherlands Institute for Radio Astronomy, Oude Hoogeveensedijk 4, 7991 PD Dwingeloo, the Netherlands

<sup>5</sup>European Space Astronomy Centre, Apartado/P.O. Box 78, Villanueva de la Canada, E-28691 Madrid, Spain

<sup>6</sup>NRAO Domenici Science Operations Center, 1003 Lopezville Road, Socorro, NM 87801

<sup>7</sup>School of Physics and Astronomy, University of Southampton, Southampton SO17 1BJ, UK

<sup>8</sup>Astronomy Department, University of Wisconsin-Madison, 475. N. Charter St., Madison, WI 53706

<sup>9</sup>Université Paris Diderot and Service d’Astrophysique, UMR AIM, CEA Saclay, F-91191 Gif-sur-Yvette, France

<sup>10</sup>NASA/Goddard Space Flight Center, Greenbelt, MD 20771

<sup>11</sup>MIT Kavli Institute for Astrophysics and Space Research, Building 37, 70 Vassar Street, Cambridge, MA 02139

<sup>12</sup>Department of Astronomy, University of Michigan, Ann Arbor, MI 48109

<sup>13</sup>Joint Institute for VLBI in Europe, Postbus 2, 7990 AA Dwingeloo, the Netherlands

<sup>14</sup>Jodrell Bank Centre for Astrophysics, School of Physics and Astronomy, University of Manchester, Manchester M13 9PL, UK

<sup>15</sup>Jansky Fellow

<sup>16</sup>Astronomical Institute of the Romanian Academy, Cutitul de Argint 5, RO-040557 Bucharest, Romania

<sup>17</sup>Research Center for Atomic Physics and Astrophysics, Atomistilor 405, RO-077125 Bucharest, Romania

<sup>18</sup>Leiden Observatory, University of Leiden, PO Box 9513, 2300 RA Leiden, the Netherlands

<sup>19</sup>Centre for Astrophysics and Supercomputing, Swinburne University of Technology, Hawthorn, 3122 Victoria, Australia

<sup>20</sup>Universities Space Research Association, Columbia, MD

<sup>21</sup>MTA Research Group for Physical Geodesy and Geodynamics, PO Box 91, H-1521 Budapest, Hungary

The 2009 November outburst of the neutron star X-ray binary Aquila X-1 was observed with unprecedented radio coverage and simultaneous pointed X-ray observations, tracing the radio emission around the full X-ray hysteresis loop of the outburst for the first time. We use these data to discuss the disc-jet coupling, finding the radio emission to be consistent with being triggered at state transitions, both from the hard to the soft spectral state and vice versa. Our data appear to confirm previous suggestions of radio quenching in the soft state above a threshold X-ray luminosity of  $\sim 10\%$  of the Eddington luminosity. We also present the first detections of Aql X-1 with Very Long Baseline Interferometry (VLBI), showing that any extended emission is relatively diffuse, and consistent with steady jets rather than arising from discrete, compact knots. In all cases where multi-frequency data were available, the source radio spectrum is consistent with being flat or slightly inverted, suggesting that the internal shock mechanism that is believed to produce optically thin transient radio ejecta in black hole X-ray binaries is not active in Aql X-1.

*Subject headings:* X-rays: binaries — radio continuum: stars — stars: individual (Aql X-1) — astrometry

## 1. Introduction

Multi-wavelength observations of accreting stellar-mass compact objects have revealed a fundamental coupling between the processes of accretion and ejection. As an X-ray binary (XRB) evolves through a set of characteristic X-ray spectral and variability states over the course of an outburst, the radio emission, assumed to arise from jets launched from the inner regions of the system, is also seen to evolve. Fender et al. (2004a) proposed a phenomenological model for this accretion-ejection (disc-jet) coupling in the relatively well-studied black hole (BH) XRBs. In this model, compact steady jets are present in the hard X-ray spectral state, with the jet power scaling with X-ray luminosity. The jet velocity increases when the source makes a transition to a softer spectral state, leading to internal shocks within the flow (e.g. Kaiser et al. 2000), observed as discrete knots of radio emission that move outwards at relativistic speeds. The compact jets then switch off. The system eventually makes a transition back to a hard spectral state, whereupon the core jets are re-established, and the source fades back into quiescence. This second state transition tends to occur at a lower luminosity than the original transition from the hard to the soft state, implying a hysteresis in the outburst cycle (Maccarone & Coppi 2003).

Compact jets are also inferred to exist in neutron star (NS) systems, from brightness temperature arguments, the observed flat-spectrum radio emission, and the detection of a jet break in broadband spectra (Migliari et al. 2006, 2010). Rapid energy transfer from the core to detached radio lobes (Fomalont et al. 2001; Fender et al. 2004a) also argues strongly for the existence of jets in NS systems, although their compact jets have not been directly imaged, as in BH systems

(Dhawan et al. 2000; Stirling et al. 2001). Since NS XRBs are typically fainter radio emitters than their BH counterparts at the same X-ray luminosity (Fender & Kuulkers 2001; Migliari & Fender 2006), the nature of the disc-jet coupling in NS systems is consequently less well understood. Migliari & Fender (2006) made a systematic study of radio emission from NS XRBs, finding evidence for steady jets in hard state systems at low luminosities ( $< 1\%$  of the Eddington luminosity,  $L_{\text{Edd}}$ ) and transient jets in outbursting sources close to  $L_{\text{Edd}}$ , as seen in BH systems but without complete suppression of the radio emission in soft states. The correlation between X-ray and radio emission in hard states was steeper in NS systems (Migliari & Fender 2006) than the analogous correlation in BH systems (Gallo et al. 2003), implying a different coupling between X-ray luminosity and mass accretion rate, although the jet power for a given accretion rate is similar in both classes of system (Körding et al. 2006).

Understanding the similarities and differences between the disc-jet coupling in BH and NS systems is crucial in determining the role played by the depth of the gravitational potential well, the stellar surface, and any stellar magnetic field in the process of jet formation.

### 1.1. Aql X-1

Aql X-1 is a recurrent transient XRB which undergoes outbursts every  $\sim 300$  d. The accretor is a confirmed NS (Koyama et al. 1981), in a  $\sim 19$ -h orbit (Chevalier & Ilovaisky 1991; Shahbaz et al. 1998; Welsh et al. 2000) with a K7V companion (Chevalier et al. 1999). Its X-ray spectral and timing behavior classify it as an atoll source (Reig et al. 2000). The distance, determined from the luminosity of its Type I X-ray bursts, is in the range 4.4–5.9 kpc (Jonker & Nelemans 2004).

Despite its frequent outbursts, there are few reported radio detections of Aql X-1, likely owing to the faintness of atoll sources in the radio band (Migliari & Fender 2006). Tudose et al. (2009a) analyzed all publicly-available archival data from the Very Large Array (VLA), taken exclusively during X-ray outbursts, between 1986 and 2005. They detected the source at 11 epochs, with a maximum radio flux density of 0.4 mJy. In all cases where multi-frequency observations were available, the radio spectrum was inverted ( $\alpha > 0$ , where flux density  $S_\nu$  scales with frequency  $\nu$  as  $S_\nu \propto \nu^\alpha$ ). They also found tentative evidence for quenching of the radio emission above a certain X-ray luminosity.

Here, we extend on the work of Tudose et al. (2009a), presenting the most complete radio coverage of an outburst of Aql X-1 obtained to date, to elucidate the nature of the radio/X-ray coupling in this source.

## 2. Observations

Rising X-ray flux from Aql X-1 was observed on 2009 November 1 (Linares et al. 2009) by the Proportional Counter Array (PCA) on board the RXTE satellite during the ongoing Galactic bulge monitoring program (Markwardt et al. 2000). Here we present follow-up radio and X-ray data taken during the outburst.

### 2.1. VLA

On detection of rising X-ray flux, we triggered VLA monitoring at 8.4 GHz. Data were taken in dual circular polarization with a total observing bandwidth of 100 MHz. The array was in its least-extended D configuration. On detection of radio emission (Sivakoff et al. 2009), we also began observing at 4.8 GHz until the source faded below our detection threshold. Further, we reduced all remaining unpublished archival VLA data, covering the outbursts of 2006 August and 2007 October. Data reduction was carried out according to standard procedures within AIPS (Greisen 2003).

### 2.2. VLBA

Following the initial VLA radio detection, we triggered observations with the Very Long Baseline Array (VLBA). We observed at 8.4 GHz in dual circular polarization, using the maximum available recording rate of 512 Mbps, corresponding to an observing bandwidth of 64 MHz per polarization. The observations, of duration 2–6 h, were phase-referenced to the nearby calibrator J1907+0127, from the third extension to the VLBA Calibrator Survey (VCS-3; Petrov et al. 2005) and located  $1.33^\circ$  from Aql X-1. The phase-referencing cycle time was 3 min, with occasional scans on the VCS-4 (Petrov et al. 2006) check source J1920-0236. For the longer observations, 30 min at the start and end of the observing run were used to observe bright calibrator sources at differing elevations to calibrate unmodeled clock and tropospheric phase errors, thereby improving the success of the phase transfer. Data reduction was carried out according to standard procedures within AIPS.

### 2.3. EVN

As reported by Tudose et al. (2009b), Aql X-1 was observed at 5 GHz with the European VLBI Network (EVN) on 2009 November 19 (14:30–19:00 UT) using the e-VLBI technique. The array comprised stations at Effelsberg, Medicina, Onsala, Torun, Westerbork, Yebes and Cambridge with a maximum recording rate of 1 Gbps. We observed in full-polarization mode with a total bandwidth of 128 MHz per polarization, and data were phase referenced to J1907+0127. The data

were calibrated in AIPS and imaged in Difmap (Shepherd 1997) using standard procedures.

## 2.4. RXTE

Following Altamirano et al. (2008), we used the 16-s time-resolution Standard 2 mode PCA data to calculate X-ray colors and intensities. Hard and soft colors were defined as the count rate ratios (9.7–16.0 keV / 6.0–9.7 keV) and (3.5–6.0 keV / 2.0–3.5 keV), respectively, and intensity was defined as the 2.0–16.0 keV count rate. Type I X-ray bursts were removed, background was subtracted and deadtime corrections were made, before normalizing intensities and colors by those of the Crab Nebula, on a per-PCU basis.

## 3. Results

### 3.1. Lightcurves

The observational results are given in Table 1 and plotted in Fig. 1, together with the publicly available 2–10 keV RXTE ASM and 15–50 keV Swift BAT lightcurves. The hard X-ray flux peaks first during the outburst, as noted by Yu et al. (2003). As this starts to decrease, the soft flux rises and the X-ray colors decrease. Radio emission is first detected at this point of X-ray spectral softening, with an 8.4 GHz flux density of  $0.68 \pm 0.09$  mJy (the highest level measured to date from Aql X-1). The hard X-ray flux then levels off while the radio emission fades below detectable levels and the soft X-ray flux peaks at  $\sim 300$  mCrab before decaying. As the X-ray color increases again and the spectrum hardens, a second burst of radio emission is detected. Thus while the radio sampling is relatively sparse during the second state transition, the radio emission is consistent with being triggered at transitions in both directions between the hard and the soft X-ray states.

### 3.2. Imaging

During the X-ray spectral softening, the source was detected for the first time with VLBI. The 5-GHz EVN observations were not fully consistent with an unresolved source, showing tentative evidence for a marginal-significance ( $\sim 3\sigma$ , 0.08 mJy) extension to the southeast (Fig. 2). The 8.4-GHz VLBA observations made on the same day were consistent with an unresolved source, to a noise level of  $0.046$  mJy beam $^{-1}$ , and implied a slightly inverted core radio spectrum ( $\alpha = 0.40 \pm 0.31$ ). Within uncertainties, the VLBI flux density was consistent at both frequencies with the integrated VLA flux density measured the previous day, so the majority of the flux was recovered on millisecond scales. However, faint extended emission at the level seen by the EVN cannot be fully discounted, since convolving the 8.4-GHz VLBA data to the 5-GHz EVN resolution raised the noise level too high to detect such emission. Simulations demonstrated that the longer baselines of

the VLBA would not detect faint extended emission as seen by the EVN on a size scale of 10 mas unless it were significantly more compact than the EVN beamsize. This allows for the possibility that the emission is sufficiently faint and extended to be resolved out by the VLBA (possibly indicative of a large-scale, steady jet), but makes it unlikely to be caused by compact, localized internal shocks. Alternatively, the extension in the EVN image may not in fact be real.

The VLBA position of Aql X-1, relative to the VCS-3 phase reference source J 1907+0127, whose position was taken to be (J 2000) 19<sup>h</sup>07<sup>m</sup>11<sup>s</sup>.9962510(747) 01°27′08″.96251(135), was

$$\begin{aligned} \text{RA} &= 19^{\text{h}}11^{\text{m}}16^{\text{s}}.0251654 \pm 0.000006 \\ \text{Dec.} &= +00^{\circ}35′05″.8920 \pm 0.0002 \quad (\text{J 2000}), \end{aligned}$$

where the quoted error bars are purely statistical errors from fitting in the image plane. Imaging the check source J 1920-0236, phase referenced to J 1907+0127, suggested that the systematic errors are well below 1 mas. This VLBA position is also consistent within errors with the EVN position.

#### 4. Discussion and comparison with black hole systems

The hardness-intensity diagram (HID) is a diagnostic plot used extensively in interpreting the X-ray evolution of BH XRB outbursts (e.g. Fender et al. 2004a). Maitra & Bailyn (2004) found that the 2000 September outburst of Aql X-1 traced out a very similar hysteresis loop in a HID to the better-studied BH candidates. Fig. 3 shows the radio emission superposed on the HID for both the 2009 November outburst of Aql X-1 and previous outbursts, showing the relation between radio emission and the X-ray spectral state of the source.

##### 4.1. The relation between X-ray state and radio emission

The radio emission is consistent with being triggered at X-ray state transitions, switching on as the source moves into the intermediate (island) state in the color-color diagram (CCD; Fig. 3), from either the hard (extreme island) or soft (banana) state. This pattern of triggering radio emission at state transitions is similar to the behavior seen in both the atoll source 4U 1728-34 (Migliari et al. 2003) and in BH XRB outbursts (Fender et al. 2004a). However, unlike in BH systems, we did not detect radio emission in the rising hard state (the right hand side of the HID), possibly due to insufficient sensitivity (our upper limits are close to the predicted values from the correlation of Migliari & Fender 2006), nor did we detect optically-thin shocked ejecta after the transition to the soft state.

The radio emission appears quenched while the system is in a high-luminosity soft (banana) state (Fig. 4). Migliari et al. (2003) and Tudose et al. (2009a) also found evidence for the quenching of the jets in NS systems above a critical X-ray luminosity, albeit on the basis of relatively sparse observational data (but see Migliari et al. 2004, for counterexamples). From Figures 3 and 4, the

critical luminosity for Aql X-1 appears to be  $\sim 0.21$  Crab, corresponding to a 2–16 keV luminosity of  $1.8 \times 10^{37} (d/5\text{kpc})^2 \text{ erg s}^{-1}$ , i.e.  $0.1L_{\text{Edd}}$  for a  $1.4M_{\odot}$  neutron star accretor. While reminiscent of the drop in radio flux seen in BH systems at a few per cent of  $L_{\text{Edd}}$  (Gallo et al. 2003), higher-sensitivity observations are required to accurately determine the critical luminosity.

## 4.2. The nature of the jets

The brightness temperature ( $T_{\text{B}}$ ) of the unresolved VLBA source is  $T_{\text{B}} > 4.3 \times 10^6 \text{ K}$ . The maximum VLA flux density of 0.68 mJy implies a source with  $r = 1.0 \times 10^4 T_{\text{B}}^{-1/2} (d/5\text{kpc}) \text{ AU}$ . Even at the inverse Compton limit of  $T_{\text{B}} = 10^{12} \text{ K}$ , the emission would arise on scales greater than the Roche lobe around the NS, which strongly suggests that the emitting material is flowing away from the system.

The two epochs with constraints on the radio spectrum are consistent with flat or slightly-inverted spectra, typically interpreted in BH XRBs as arising from partially self-absorbed compact jets (Blandford & Königl 1979). Reduction of archival VLA data (Table 1 and Tudose et al. 2009a) showed that every dual-frequency detection of the source to date is consistent with a flat or inverted radio spectrum, albeit with fairly large error bars. Reducing the error bars by taking a weighted mean of all spectral indices taken outside the hard (extreme island) X-ray state (in which, by analogy with BH, a flat spectrum is expected) gives  $\alpha = 0.05 \pm 0.16$ . Such a flat spectrum is also consistent with the lack of optically-thin ejecta in the VLBI observations, and with the recovery of the full integrated VLA flux with the VLBA and EVN. We thus find no evidence for transient, optically thin jet emission as seen in BH XRB outbursts.

If confirmed by future observations, the marginal EVN extension would imply a jet of size  $\sim 10 \text{ mas}$  ( $< 50(d/5\text{kpc}) \text{ AU}$ ). If not, the VLBA beamsize of  $2.9 \times 1.1 \text{ mas}^2$  gives an upper limit on the physical size scale of the jets of  $< 15(d/5\text{kpc}) \text{ AU}$  at 8.4 GHz. Such a small size is consistent with the low flux density, when compared to the case of Cyg X-1 (Heinz 2006).

Only two NS XRBs, Sco X-1 and Cir X-1, have previously been imaged on VLBI scales. Fomalont et al. (2001) detected resolved radio lobes in Sco X-1, which moved out from the central source at speeds of 0.3–0.6 $c$ . Rather than being internal shocks within a jet, these were interpreted as the working surfaces where the jets impacted the surrounding environment. From the time delay between corresponding flaring events in the core and these hotspots, it was inferred that an unseen beam transferred energy between the core and the lobes at a velocity  $> 0.95c$ . Limits on the jet size in Cir X-1 were derived by Preston et al. (1983) and Phillips et al. (2007), and although scatter-broadened, it was speculated that a compact jet of size 35 mas ( $175(d/5\text{kpc}) \text{ AU}$ ) might be present in the system. While Sco X-1 is a Z-source, Cir X-1 shows characteristics of both atoll and Z-sources (Oosterbroek et al. 1995), and Aql X-1 is an atoll source, none of them show clear evidence for internal shocks propagating down the jets at relativistic speeds and giving rise to discrete radio knots, as seen in BH outbursts. While approximate mass scalings would suggest

that optically-thin NS jets should be less bright than those in BH, they should be detectable, albeit on smaller scales. Thus the mechanism responsible for generating internal shocks (variations in the jet Lorentz factor are often invoked) is either less effective in NS XRBs than in their BH counterparts, or the shocks are less efficient emitters. Possible explanations include a less variable or more smoothly varying outflow speed (although NS jets can produce ultrarelativistic outflows; Fender et al. 2004b), a high sound speed (although with a maximum of  $c/\sqrt{3}$ , this appears unlikely if all NS jets are highly relativistic), or a high magnetic field to smooth out variations in the flow (possible, given the existing stellar field). More speculatively, should the discrete knots be ballistic ejecta launched from magnetic fields threading the ergosphere (Blandford & Znajek 1977; Punsly & Coroniti 1990), rather than internal shocks, this mechanism would not be present in NS systems. Disk fields (Blandford & Payne 1982) would then be the best candidate for accelerating the NS and hard state BH jets, as suggested by Meier (2003).

Further sensitive, high-resolution radio observations of NS sources in outburst are required to confirm this lack of transient ejecta and ascertain whether this is indeed a fundamental difference between NS and BH jets. Similarities and differences between the two classes of source will constrain the role of the stellar surface and magnetic field and the depth of the potential well in accelerating relativistic jets from accreting compact objects.

## 5. Conclusions

We have obtained unprecedented radio coverage of an outburst of the NS XRB Aql X-1, demonstrating that the radio emission is consistent with being activated by both transitions from a hard state to a soft state and by the reverse transition at lower X-ray luminosity. Our data appear to confirm previous suggestions of quenched radio emission above a certain X-ray luminosity, corresponding to  $\sim 10\%$  of the Eddington luminosity. We have for the first time detected the source with VLBI, which together with the measured brightness temperature, radio spectra and integrated flux density observed by the VLA demonstrates that the radio emission in this source is consistent with the compact, partially self-absorbed steady jets seen in the hard states of BH XRBs. NSs thus appear equally capable of launching jets as BHs, but the absence of bright, optically thin, relativistically moving knots may suggest a fundamental difference in the jet formation process between NS and BH systems, possibly hinting at an additional role from the ergosphere.

J.C.A.M.-J. is a Jansky Fellow of the National Radio Astronomy Observatory (NRAO). M.L. is supported by the Netherlands Organisation for Scientific Research (NWO). D.M.R. acknowledges support from a NWO Veni Fellowship. The VLA and VLBA are facilities of the NRAO which is operated by Associated Universities, Inc., under cooperative agreement with the National Science Foundation. The European VLBI Network is a joint facility of the European, Chinese, South African and other radio astronomy institutes funded by their national research councils. e-VLBI developments in Europe were supported by the EC DG-INFSO funded Communication Network

Developments project ‘EXPREs’. Quick-look RXTE results provided by the ASM/RXTE team. Swift/BAT transient monitor results provided by the Swift/BAT team.

*Facilities:* Swift, RXTE, VLA, VLBA, EVN

## REFERENCES

- Altamirano, D., van der Klis, M., Méndez, M. and, Jonker, P. G., Klein-Wolt, M., & Lewin, W. H. G. 2008, *ApJ*, 685, 436
- Blandford, R. D., Königl, A. 1979, *ApJ*, 232, 34
- Blandford, R. D., & Payne, D. G. 1982, *MNRAS*, 199, 883
- Blandford, R. D., & Znajek, R. L. 1977, *MNRAS*, 179, 433
- Chevalier, C., & Ilovaisky, S. A. 1991, *A&A*, 251, L11
- Chevalier, C., Ilovaisky, S. A., Leisy, P., & Patat, F. 1999, *A&A*, 347, L51
- Dhawan, V., Mirabel, I. F., & Rodríguez, L. F. 2000, *ApJ*, 543, 373
- Fender, R. P., & Kuulkers, E. 2001, *MNRAS*, 324, 923
- Fender, R. P., Belloni, T. M., & Gallo, E. 2004a, *MNRAS*, 355, 1105
- Fender, R., Wu, K., Johnston, H., Tzioumis, T., Jonker, P., Spencer, R., & van der Klis, M. 2004b, *Nature*, 427, 222
- Fomalont, E. B., Geldzahler, B. J., & Bradshaw, C. F. 2001, *ApJ*, 558, 283
- Gallo, E., Fender, R. P., & Pooley, G. G. 2003, *MNRAS*, 344, 60
- Greisen E. W. 2003, in *Information Handling in Astronomy: Historical Vistas*, ed. A. Heck (Dordrecht: Kluwer), 109
- Heinz, S. 2006, *ApJ*, 636, 316
- Jonker, P. G., & Nelemans, G. 2004, *MNRAS*, 354, 355
- Kaiser, C. R., Sunyaev, R., & Spruit, H. C. 2000, *A&A*, 356, 975
- Körding, E. G., Fender, R. P., & Migliari, S. 2006, *MNRAS*, 369, 1451
- Koyama, K., et al. 1981, *ApJ*, 247, L27
- Linares, M., et al. 2009, *The Astronomer’s Telegram*, 2288

- Maccarone, T. J., & Coppi, P. S. 2003, MNRAS, 338, 189
- Maitra, D., & Bailyn, C. D. 2004, ApJ, 608, 444
- Markwardt, C. B., Swank, J. H., Marshall, F. E., & in 't Zand, J. J. M. 2000, in 'Rossi2000: Astrophysics with the Rossi X-ray Timing Explorer', E7
- Meier, D. L. 2003, New Astronomy Reviews, 47, 667
- Migliari, S., & Fender, R. P. 2006, MNRAS, 366, 79
- Migliari, S., Fender, R. P., Rupen, M., Jonker, P. G., Klein-Wolt, M., Hjellming, R. M., & van der Klis, M. 2003, MNRAS, 342, L67
- Migliari, S., Fender, R. P., Rupen, M., Wachter, S., Jonker, P. G., Homan, J., & van der Klis, M. 2004, MNRAS, 351, 186
- Migliari, S., Tomsick, J. A., Maccarone, T. J., Gallo, E., Fender, R. P., Nelemans, G., & Russell, D. M. 2006, ApJ, 643, L41
- Migliari, S., et al. 2010, ApJ, 710, 117
- Oosterbroek, T., van der Klis, M., Kuulkers, E., van Paradijs, J., & Lewin, W. H. G. 1995, A&A, 297, 141
- Petrov, L., Kovalev, Y. Y., Fomalont, E., & Gordon, D. 2005, AJ, 129, 1163
- Petrov, L., Kovalev, Y. Y., Fomalont, E. B., & Gordon, D. 2006, AJ, 131, 1872
- Phillips, C. J., et al. 2007, MNRAS, 380, L11
- Preston, R. A., Morabito, D. D., Wehrle, A. E., Jauncey, D. L., Batty, M. J., Haynes, R. F., Wright, A. E., & Nicolson, G. D. 1983, ApJ, 268, L23
- Punsly, B., & Coroniti, F. V. 1990, ApJ, 354, 583
- Reig, P., Méndez, M., van der Klis, M., & Ford, E. C. 2000, ApJ, 530, 916
- Shahbaz, T., Thorstensen, J. R., Charles, P. A., & Sherman, N. D. 1998, MNRAS, 296, 1004
- Shepherd M.C. 1997, in ASP Conf. Ser. Vol. 125, Astronomical Data Analysis Software and Systems VI., eds. G. Hunt and H.E. Payne (San Francisco: Astron. Soc. Pac.), 77
- Sivakoff, G. R., Miller-Jones, J., Fox, O., Linares, M., Altamirano, D., & Russell, D. 2009, The Astronomer's Telegram, 2302
- Stirling, A. M., Spencer, R. E., de la Force, C. J., Garrett, M. A., Fender, R. P., & Ogle, R. N. 2001, MNRAS, 327, 1273

- Tudose, V., Fender, R. P., Linares, M., Maitra, D., & van der Klis, M. 2009a, MNRAS, 400, 2111
- Tudose, V., Paragi, Z., Miller-Jones, J., Garrett, M., Fender, R., Rushton, A., & Spencer, R. 2009b, The Astronomer's Telegram, 2317
- Welsh, W. F., Robinson, E. L., & Young, P., 2000, AJ, 120, 943
- Yu, W., Klein-Wolt, M., Fender, R., & van der Klis, M. 2003, ApJ, 589, L33

---

This preprint was prepared with the AAS L<sup>A</sup>T<sub>E</sub>X macros v5.2.

<sup>1</sup><http://swift.gsfc.nasa.gov/docs/swift/results/transients/AqlX-1.lc.txt>

<sup>2</sup><http://xte.mit.edu/XTE/asmlc/srcs/aqlx1.html>

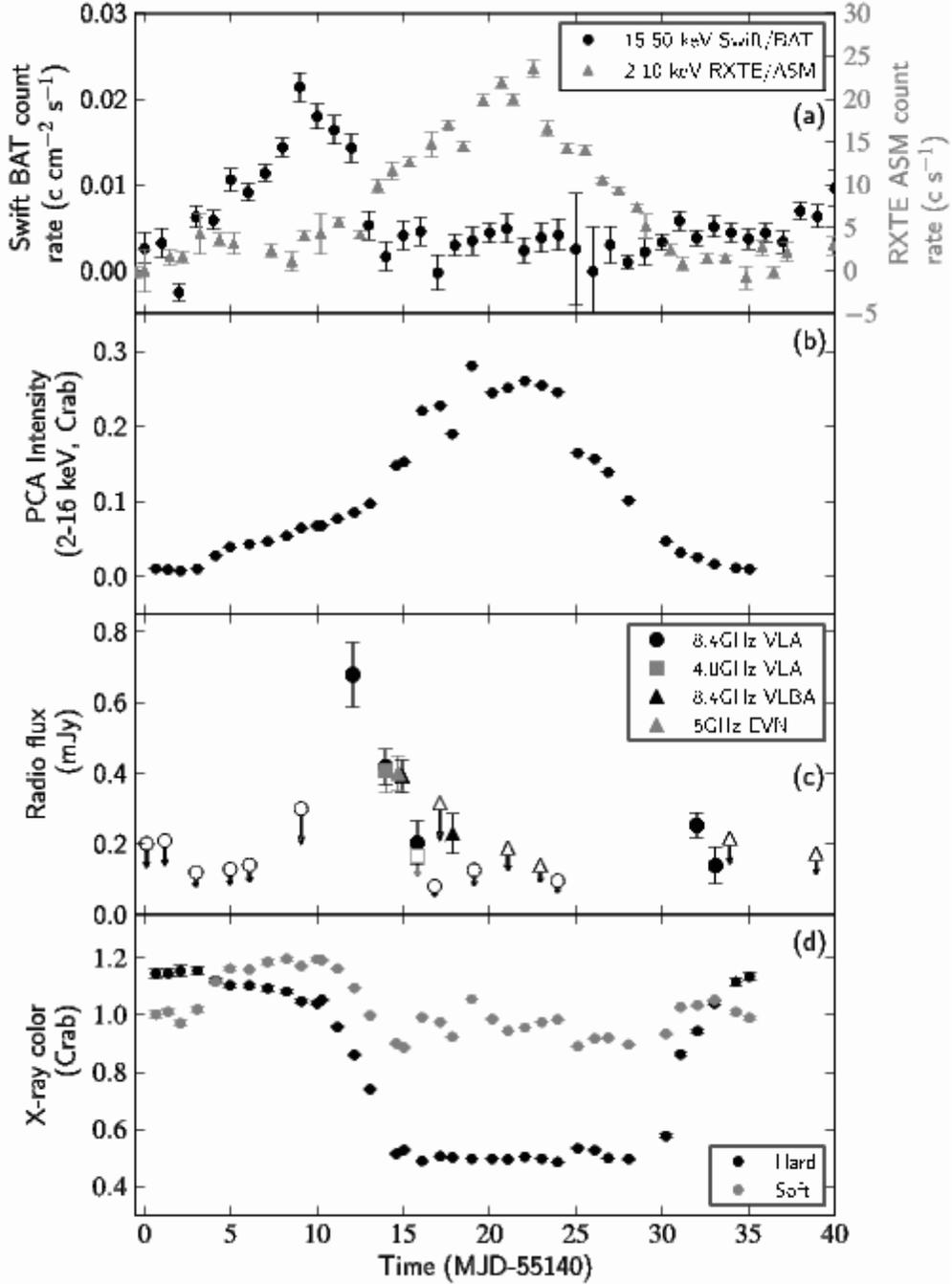


Fig. 1.— Radio and X-ray lightcurves of the 2009 November outburst of Aql X-1. (a) Swift BAT count rate<sup>1</sup> in black (left-hand axis) and RXTE ASM count rate<sup>2</sup> in grey (right-hand axis). (b) RXTE PCA intensity. (c) Radio flux density. Circles and squares indicate VLA observations and triangles VLBI observations. Black and grey markers denote 8.4 and 5 GHz observations, respectively. Filled markers denote detections and corresponding open markers the  $3\sigma$  upper limits. (d) X-ray colors, defined as in Section 2.4. Note the radio detections at the state transitions where the hard X-ray color changes.

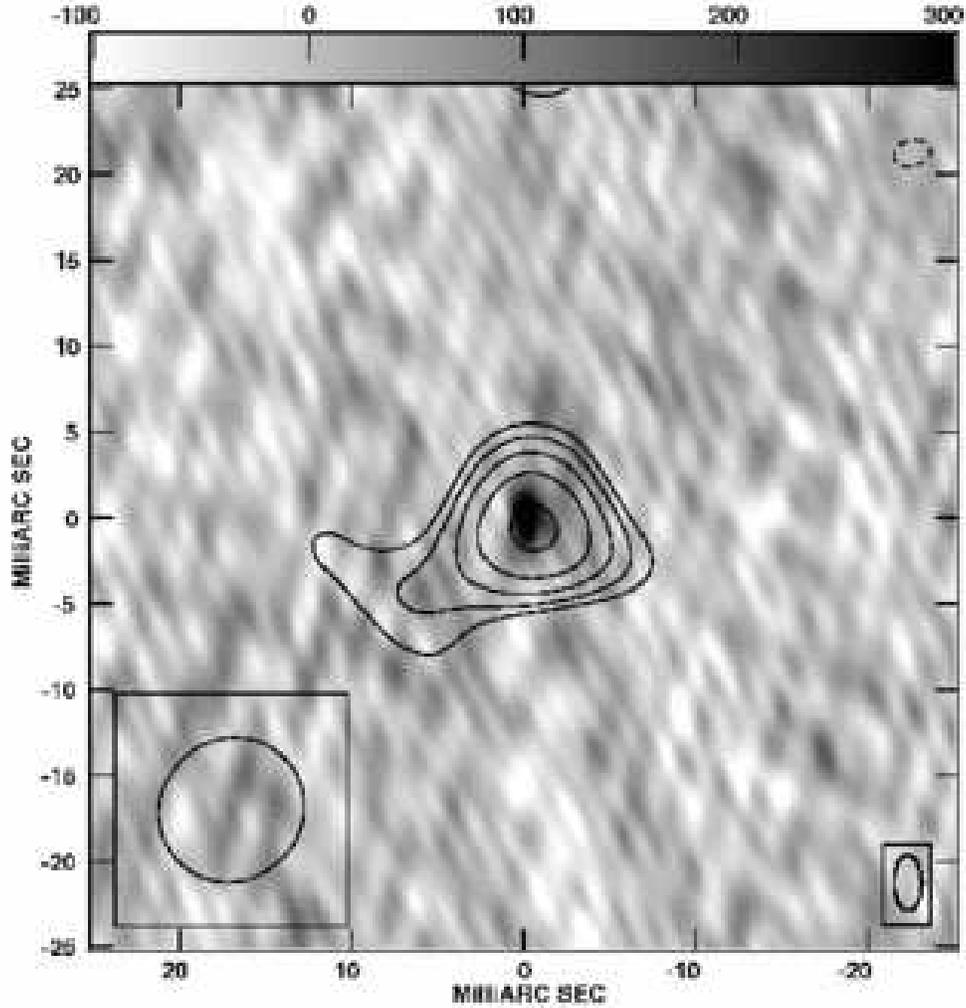


Fig. 2.— Greyscale 8.4-GHz VLBA image of Aql X-1 from 2009 November 19 (MJD 55154–55155), with 5-GHz EVN contours overlaid. Contours are at levels of  $\pm(\sqrt{2})^n$  times the rms noise level of 37 microJy/beam, where  $n = 2, 3, 4, \dots$ . EVN and VLBA beamsizes are shown at lower left and right, respectively. Note the marginal ( $\sim 3\sigma$ ) extension to the southeast in the EVN image. No corresponding extension is seen with the VLBA.

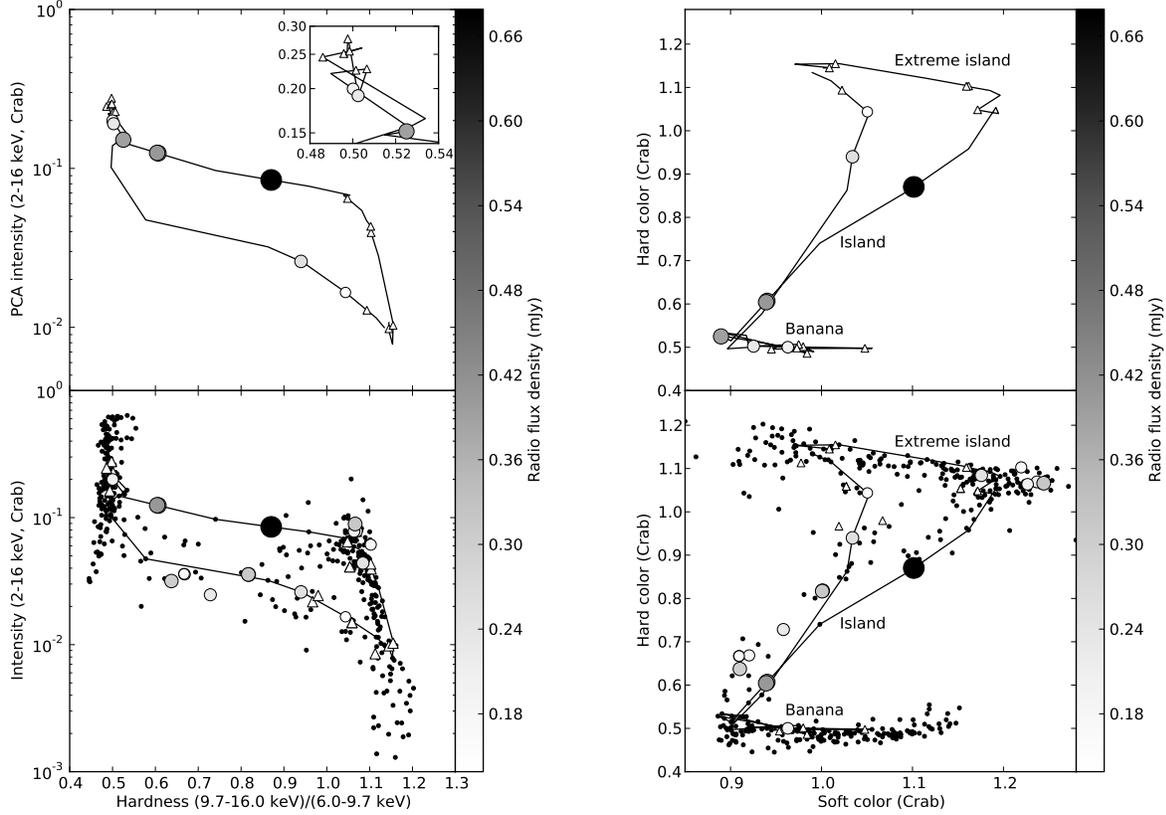


Fig. 3.— Left: HIDs for the 2009 November outburst of Aql X-1 (top) and all recorded outbursts with archival PCA data (bottom). Right: Color-color diagrams (CCDs) for the 2009 November outburst (top) and the archival outbursts (bottom). During the 2009 outburst, the source moves anticlockwise around the HID hysteresis loop and clockwise around the CCD track (solid lines in both figures). The X-ray state at the time of the radio observations has been interpolated from X-ray observations within 2 d. Circles indicate radio detections at either 5 or 8.4 GHz, with the VLA, VLBA or EVN. The size and color of the circles represent the radio flux density, according to the scale shown on the right of the plots. Open triangles denote radio upper limits. Dots show RXTE PCA measurements without simultaneous radio observations. The inset in the top HID shows a zoomed-in version of the soft state (upper left corner of the HID). Radio data from previous outbursts are taken from Tudose et al. (2009a) and Table 1. These plots show how the radio emission corresponds to the X-ray state of the source.



Table 1. X-ray and radio observations of Aql X-1.

Date	MJD PCA (day)	PCA flux (mCrab)	Hard color <sup>a</sup>	Soft color <sup>b</sup>	MJD VLA (day)	8.4 GHz VLA flux (mJy)	4.8 GHz VLA flux (mJy)	MJD VLBA (day)	8.4 GHz VLBA flux (mJy)	5.0 GHz EVN flux (mJy)	X-ray state <sup>c</sup>
2006 May 28	...	...	...	...	53883.57	...	< 0.17	...	...	...	...
2006 May 30	...	...	...	...	53885.36	...	0.46 ± 0.08	...	...	...	...
2006 Aug 02	53949.41	24.65 ± 0.06	0.729 ± 0.008	0.958 ± 0.006	53949.41	0.23 ± 0.05	0.25 ± 0.06	...	...	...	IS
2006 Aug 03	53950.34	33.10 ± 0.10	0.621 ± 0.009	0.902 ± 0.006	53950.21	0.30 ± 0.04	...	...	...	...	IS
2006 Aug 04	53951.45	37.25 ± 0.04	0.694 ± 0.004	0.930 ± 0.003	53951.06	0.18 ± 0.04	...	...	...	...	IS
2006 Aug 07	53954.20	36.91 ± 0.05	0.801 ± 0.004	0.993 ± 0.003	53954.38	0.31 ± 0.04	0.31 ± 0.07	...	...	...	IS
2006 Aug 09	53955.97	26.25 ± 0.06	0.966 ± 0.008	1.074 ± 0.006	53956.27	< 0.11	...	...	...	...	IS
2006 Aug 11	53958.06	15.46 ± 0.03	1.062 ± 0.007	1.024 ± 0.005	53958.34	< 0.08	< 0.11	...	...	...	EIS
2006 Aug 18	53965.46	7.82 ± 0.02	1.119 ± 0.013	0.966 ± 0.007	53965.28	< 0.12	...	...	...	...	EIS
2006 Aug 21	...	...	...	...	53968.34	< 0.14	< 0.18	...	...	...	...
2006 Aug 23	...	...	...	...	53970.33	< 0.14	< 0.23	...	...	...	...
2006 Aug 28	...	...	...	...	53975.32	< 0.12	...	...	...	...	...
2006 Aug 31	...	...	...	...	53978.21	< 0.10	...	...	...	...	...
2007 May 22	54242.41	39.53 ± 0.06	1.064 ± 0.006	1.156 ± 0.005	54242.59	< 0.24	< 0.66	...	...	...	EIS
2007 Sep 28	...	...	...	...	54371.05	0.28 ± 0.04	0.29 ± 0.05	...	...	...	...
2007 Sep 30	...	...	...	...	54373.87	0.37 ± 0.09	...	...	...	...	...
2007 Oct 02	54376.99	13.88 ± 0.05	1.081 ± 0.014	1.026 ± 0.009	54375.99	0.16 ± 0.05	< 0.18	...	...	...	EIS
2007 Oct 06	54379.87	9.60 ± 0.04	1.116 ± 0.019	0.971 ± 0.010	54379.17	< 0.10	< 0.12	...	...	...	EIS
2007 Oct 07	...	...	...	...	54380.85	< 0.18	< 0.24	...	...	...	...
2007 Oct 19	...	...	...	...	54392.99	< 0.14	< 0.18	...	...	...	...
2009 Nov 05	55140.67	10.71 ± 0.04	1.145 ± 0.015	1.002 ± 0.011	55140.12	< 0.20	...	...	...	...	EIS
2009 Nov 06	55141.38	9.48 ± 0.03	1.145 ± 0.013	1.011 ± 0.009	55141.19	< 0.21	...	...	...	...	EIS
2009 Nov 07	55142.09	7.83 ± 0.04	1.154 ± 0.019	0.971 ± 0.011	...	...	...	...	...	...	EIS
2009 Nov 08	55143.07	10.54 ± 0.03	1.155 ± 0.012	1.019 ± 0.008	55142.99	< 0.12	...	...	...	...	EIS
2009 Nov 09	55144.12	28.06 ± 0.05	1.121 ± 0.007	1.116 ± 0.006	...	...	...	...	...	...	EIS
2009 Nov 09	55144.97	39.46 ± 0.06	1.103 ± 0.005	1.162 ± 0.005	55144.97	< 0.13	...	...	...	...	EIS
2009 Nov 11	55146.08	43.19 ± 0.05	1.103 ± 0.004	1.159 ± 0.004	55146.09	< 0.14	...	...	...	...	EIS
2009 Nov 12	55147.14	46.97 ± 0.13	1.093 ± 0.010	1.185 ± 0.009	...	...	...	...	...	...	EIS
2009 Nov 13	55148.25	54.30 ± 0.09	1.082 ± 0.006	1.196 ± 0.006	...	...	...	...	...	...	EIS
2009 Nov 14	55149.09	64.88 ± 0.09	1.048 ± 0.005	1.171 ± 0.005	55149.08	< 0.30	...	...	...	...	EIS
2009 Nov 15	55150.00	67.76 ± 0.13	1.040 ± 0.006	1.195 ± 0.007	...	...	...	...	...	...	EIS
2009 Nov 15	55150.28	67.87 ± 0.07	1.054 ± 0.004	1.192 ± 0.003	...	...	...	...	...	...	EIS
2009 Nov 16	55151.19	77.27 ± 0.06	0.958 ± 0.003	1.162 ± 0.002	...	...	...	...	...	...	IS

Table 1—Continued

Date	MJD PCA (day)	PCA flux (mCrab)	Hard color <sup>a</sup>	Soft color <sup>b</sup>	MJD VLA (day)	8.4 GHz VLA flux (mJy)	4.8 GHz VLA flux (mJy)	MJD VLBA (day)	8.4 GHz VLBA flux (mJy)	5.0 GHz EVN flux (mJy)	X-ray state <sup>c</sup>
2009 Nov 17	55152.17	85.42 ± 0.08	0.860 ± 0.003	1.095 ± 0.003	55152.07	0.68 ± 0.09	...	...	...	...	IS
2009 Nov 18	55153.08	96.99 ± 0.11	0.740 ± 0.003	0.998 ± 0.003	...	...	...	...	...	...	IS
2009 Nov 19	55154.60	148.00 ± 0.25	0.515 ± 0.004	0.900 ± 0.004	55154.00	0.42 ± 0.05	0.41 ± 0.06	55154.94	0.39 ± 0.05	0.40 ± 0.05 <sup>d</sup>	IS
2009 Nov 20	55155.04	152.59 ± 0.10	0.528 ± 0.002	0.886 ± 0.001	55155.81	0.20 ± 0.06	< 0.17	...	...	...	BS
2009 Nov 21	55156.09	220.63 ± 0.13	0.490 ± 0.001	0.992 ± 0.001	55156.82	< 0.08	...	...	...	...	BS
2009 Nov 22	55157.14	227.52 ± 0.11	0.507 ± 0.001	0.975 ± 0.001	...	...	...	55157.12	< 0.32	...	BS
2009 Nov 22	55157.85	189.97 ± 0.20	0.503 ± 0.002	0.923 ± 0.002	...	...	...	55157.86	0.23 ± 0.06	...	BS
2009 Nov 23	55158.97	280.73 ± 0.21	0.498 ± 0.002	1.055 ± 0.002	...	...	...	...	...	...	BS
2009 Nov 24	...	...	...	...	55159.10	< 0.13	...	...	...	...	BS
2009 Nov 25	55160.15	244.67 ± 0.20	0.497 ± 0.002	0.985 ± 0.002	...	...	...	...	...	...	BS
2009 Nov 26	55161.07	251.19 ± 0.14	0.496 ± 0.001	0.945 ± 0.001	...	...	...	55161.06	< 0.19	...	BS
2009 Nov 27	55162.05	260.50 ± 0.14	0.504 ± 0.001	0.956 ± 0.001	...	...	...	55162.94	< 0.14	...	BS
2009 Nov 28	55163.03	254.56 ± 0.14	0.498 ± 0.001	0.975 ± 0.001	...	...	...	...	...	...	BS
2009 Nov 28	55163.94	245.53 ± 0.13	0.486 ± 0.001	0.984 ± 0.001	55163.94	< 0.10	...	...	...	...	BS
2009 Nov 30	55165.12	164.62 ± 0.11	0.534 ± 0.002	0.891 ± 0.001	...	...	...	...	...	...	BS
2009 Dec 01	55166.10	156.87 ± 0.10	0.527 ± 0.002	0.917 ± 0.001	...	...	...	...	...	...	BS
2009 Dec 01	55166.88	138.99 ± 0.11	0.500 ± 0.002	0.920 ± 0.002	...	...	...	...	...	...	BS
2009 Dec 03	55168.06	101.59 ± 0.09	0.497 ± 0.002	0.896 ± 0.002	...	...	...	...	...	...	BS
2009 Dec 05	55170.22	47.42 ± 0.09	0.577 ± 0.005	0.934 ± 0.004	...	...	...	...	...	...	IS
2009 Dec 06	55171.07	32.09 ± 0.04	0.863 ± 0.004	1.028 ± 0.003	...	...	...	...	...	...	IS
2009 Dec 07	55172.05	25.72 ± 0.04	0.944 ± 0.006	1.034 ± 0.004	55172.01	0.25 ± 0.04	...	...	...	...	IS
2009 Dec 08	55173.03	16.86 ± 0.03	1.040 ± 0.008	1.052 ± 0.006	55173.09	0.14 ± 0.05	...	55173.92	< 0.22	...	EIS
2009 Dec 09	55174.28	11.47 ± 0.04	1.115 ± 0.013	1.010 ± 0.008	...	...	...	...	...	...	EIS
2009 Dec 10	55175.06	9.96 ± 0.03	1.134 ± 0.014	0.990 ± 0.008	...	...	...	...	...	...	EIS
2009 Dec 13	...	...	...	...	...	...	...	55178.92	< 0.17	...	EIS

<sup>a</sup>Count rate ratio (9.7–16.0 keV / 6.0–9.7 keV)<sup>b</sup>Count rate ratio (3.5–6.0 keV / 2.0–3.5 keV)<sup>c</sup>EIS, IS and BS denote extreme island state, island state, and banana state, respectively, defined from RXTE observations within 2 d of the radio data.<sup>d</sup>The MJD of the EVN observation was 55154.70.